

Robust Position Control of Ultrasonic Motor Considering Dead-Zone

Shogo Odomari¹, Araz Darba¹, Kosuke Uchida¹, Tomonobu Senjyu¹, and Atsushi Yona¹

¹Department of Electrical and Electronics Engineering, University of the Ryukyus, Japan

E-mail: b985542@tec.u-ryukyu.ac.jp

Abstract—Intrinsic properties of ultrasonic motor (high torque for low speed, high static torque, compact in size, etc.) offer great advantages for industrial applications. However, when load torque is applied, dead-zone occurs in the control input. Therefore, a nonlinear controller, which considers dead-zone, is adopted for ultrasonic motor. The state quantities, such as acceleration, speed, and position are needed to apply the nonlinear controller for position control. However, rotary encoder causes quantization errors in the speed information. This paper presents a robust position control method for ultrasonic motor considering dead-zone. The state variables for nonlinear controller are estimated by a Variable Structure System(VSS) observer. Besides, a small, low cost, and good response nonlinear controller is designed by using a micro computer that is essential in embedded system for the developments of industrial equipments. Effectiveness of the proposed method is verified by the experimental results.

I. INTRODUCTION

In recent years, ultrasonic motor(USM) is gaining attention as it has good characteristics and is small in size. The drive source of ultrasonic motor is ultrasonic vibration of piezoelectric element. USM is expected to be applied to robot actuator, high precision positioning and medical equipments[1]. The operating principle of an USM has complicated speeds characteristics compared to a conventional electromagnetic motor which makes it a special kind of motor.

However, an USM has dead-zone in its control input with applied load torque[3]. Since H_∞ controller is a linear controller[2], it cannot control the USM with unknown dead-zone. Therefore, nonlinear controller[4]-[6], which is not used dead-zone inverse, is used for robust position control of USM with unknown dead-zone. To apply nonlinear controller for position control of USM, state variables such as acceleration, speed and position of the USM are needed. Speed information detected by a rotary encoder have quantization errors, especially in low speed region. Therefore, to estimate actual rotor speed accurately, a VSS observer[7] is proposed with the possibility of decreasing quantization error.

Essential industrial equipments are developed in small size, lightweight and power-saving technology, by using embedded system. Usage of micro computer in embedded system, has advantages(such as it can discretize all processing, can design stable and small size circuit in comparison to analog circuit, can construct

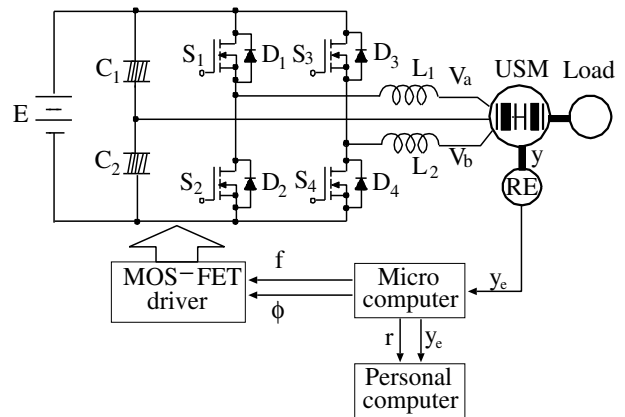


Fig. 1 Drive system of USM.

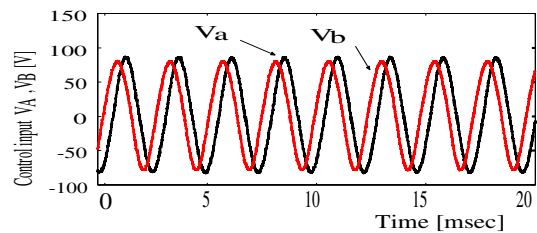


Fig. 2 Output voltages of two-phase inverter.

control system at low cost, can upgrade response, and can make the system design easily).

This paper presents a digital implementation[8]-[10] of a nonlinear controller and a VSS observer by using a micro computer for efficient position control of the USM with unknown dead-zone. The state variables are estimated by the VSS observer and are used in nonlinear controller. The proposed nonlinear controller is found satisfactory.

II. SYSTEM CONFIGURATION

A. Driving system of USM

Configuration of the USM control system used in this study is shown in Fig. 1. The USM used in the experiment is a traveling wave USM(SHINSEI CORPORATION : USR-60). Output voltages of the two-phase inverter are shown in Fig. 2. A traveling wave is formed on the stator surface when this voltage is applied to the stator, the rotor moves, and USM turns to the opposite direction of the traveling wave.

Table 1. Design specifications of USM.

Drive frequency	40 kHz
Drive voltage	100 V _{rms}
Rated current	53 mA/phase
Rated torque	0.314 Nm
Rated output power	3 W
Rated speed	9.0 rad/s
Mass	0.240 kg

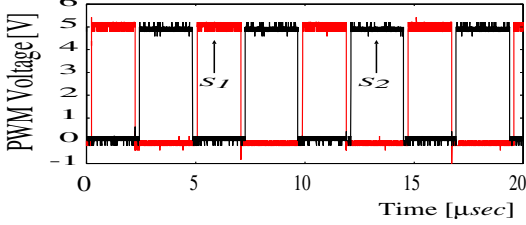


Fig. 3 PWM signal.

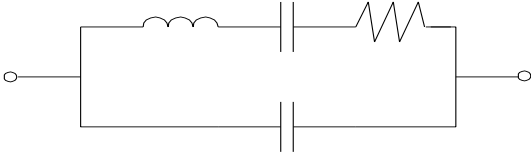


Fig. 4 Equivalent circuit of USM.

Specifications of the USM is shown in Table 1. An electromagnetic brake of the load and the rotary encoder are connected by a coupling. Electromagnetic brake is used to apply the load torque when voltage is applied. The rotary encoder is used for detecting the produced pulse in proportion to angle of the rotation of the motor shaft. Micro controller detects the rotor position for pulse number by rotary encoder(10,000 pulse/rev.). Reference position r and measured position y_e of the USM are recorded. There are two control methods of USM: driving frequency control and applied voltage phase difference control. In position control of the USM, applied voltage phase difference control has higher efficiency than driving frequency control. In this study, we use applied voltage phase difference control, and the driving frequency f is constant at 41 kHz.

B. Driving circuit configuration

Power MOS-FET are used as switching device. The USM is a large capacitive load by looked from the inverter side. For improved efficiency by decreasing capacitive load, intercalate inductances are set in series.

In PWM signal to generate micro computer input to inverter circuit, short to switch on both arm of tops and bottoms, braking of switching devices by over current, we should input PWM signals with off time to both arms(dead time). Generated PWM signals with dead time are shown in Fig. 3. In Fig. 3, to generate dead time in input signal to switching device S1 and S2 can check. The inverter produces rectangular wave forms with these PWM signals. However, we can

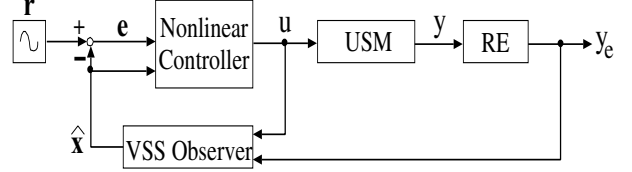


Fig. 5 System configuration.

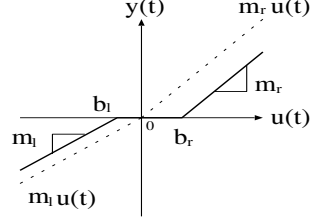


Fig. 6 Dead-zone model.

get sinusoidal voltage by making resonance with the equivalent circuit of the USM as shown in Fig. 4.

III. CONTROL ALGORITHM

System configuration in this study is shown in Fig. 5. This section is designed nonlinear controller and VSS observer.

A. Dead-zone model

Dead-zone model is shown in Fig. 6 and mathematical equation is given as follows.

$$y(t) = \begin{cases} m_r(u(t) - b_r) & b_r \leq u(t), \\ 0 & b_l < u(t) < b_r, \\ m_l(u(t) - b_l) & u(t) \leq b_l, \end{cases} \quad (1)$$

This equation is rewritten as

$$y(t) = mu(t) + d(u(t)), \quad (2)$$

where,

$$m = \begin{cases} m_r & 0 \leq u(t), \\ m_l & u(t) < 0, \end{cases} \quad (3)$$

$$d(u(t)) = \begin{cases} -m_r b_r & b_r \leq u(t), \\ -m_r u(t) & 0 \leq u(t) < b_r, \\ -m_l u(t) & b_l < u(t) < 0, \\ -m_l b_l & u(t) \leq b_l. \end{cases} \quad (4)$$

B. Nonlinear controller design

Nonlinear system for position control of USM is given as follows.

$$\begin{aligned} x^{(3)}(t) + 2\zeta\omega_n\ddot{x} + \omega_n^2\dot{x}, \\ = x^{(3)}(t) + a_3\ddot{x} + a_2\dot{x}, \\ = \omega_n^2 K_f y(t) = bmu(t) + bd(u(t)), \end{aligned} \quad (5)$$

where, $\mathbf{a} = [a_1 \ a_2 \ a_3] = [0 \ \omega_n^2 \ 2\zeta\omega_n]$, $b = \omega_n^2 K_f$. The filter tracking error is defined as

$$s(t) = \left(\frac{d}{dt} + \lambda \right)^{n-1} \mathbf{e}(t) = \mathbf{\Lambda}^T \mathbf{e}(t), \quad (6)$$

where, $\Lambda^T = [\lambda^2 \ 2\lambda \ 1]$, $e(t) = r(t) - x(t)$. If we define $\Lambda_v^T = [0 \ \lambda^2 \ 2\lambda]$, the filter tracking error differential equation is given as follows.

$$\begin{aligned} \dot{s}(t) &= \Lambda_v^T e(t) + e^{(3)}(t), \\ &= \Lambda_v^T e(t) + a_3 \ddot{x} + a_2 \dot{x} \\ &\quad - bmu(t) - bd(u(t)) + r^{(3)}(t). \end{aligned} \quad (7)$$

It should satisfy $s(t)\dot{s}(t) \leq -M|s(t)|$ to keep $s(t) = 0$ which leads to ideal control input of Eq. (8).

$$\begin{aligned} u(t) &= k_d s(t) + \frac{1}{bm}(r^{(3)}(t) + \Lambda_v^T e(t)) + \frac{a_3}{bm} \ddot{x} \\ &\quad + \frac{a_2}{bm} \dot{x} - \frac{d(u(t))}{m} + M \text{sgn}(s(t)), \end{aligned} \quad (8)$$

where k_d is a constant and M is the positive constant. We obtain the following equation when we rewrite Eq. (7) using Eq. (8).

$$\begin{aligned} \dot{s}(t) &= u_d(t) + a_3 \ddot{x} + a_2 \dot{x} - bd(u(t)) \\ &\quad - bm \left[k_d s(t) + \frac{u_d(t)}{bm} + \frac{a_3}{bm} \ddot{x} \right. \\ &\quad \left. + \frac{a_2}{bm} \dot{x} - \frac{d(u(t))}{m} + M \text{sgn}(s(t)) \right]. \end{aligned} \quad (9)$$

where, $u_d = r^{(3)}(t) + \Lambda_v^T e(t)$.

Next, Lyapunov function is selected as follows.

$$V_c(t) = \frac{1}{2bm} s^2(t). \quad (10)$$

Differentiating the equation, we have

$$\begin{aligned} \dot{V}_c(t) &= \frac{1}{bm} s \dot{s}, \\ &= \frac{u_d s(t)}{bm} + \frac{s(t)}{bm} (a_3 \ddot{x} + a_2 \dot{x}) - \frac{d(u(t))s(t)}{m} \\ &\quad - s(t) \left[k_d s(t) + \frac{u_d}{bm} + \frac{a_3}{bm} \ddot{x} + \frac{a_2}{bm} \dot{x} \right. \\ &\quad \left. - \frac{d(u(t))}{m} + M \text{sgn}(s(t)) \right], \\ &= -k_d s^2(t) - M|s(t)| \leq -k_d s^2(t). \end{aligned} \quad (11)$$

Therefore if $k_d > 0$ and Lyapunov function is negative, nonlinear controller can be stable.

C. Design of VSS observer

This section discusses the design of a VSS observer. The continuous time system can be presented as

$$\begin{aligned} \dot{x}(t) &= Ax(t) + Bh(t) + Bu(t), \\ y(t) &= Cx(t). \end{aligned} \quad (12)$$

where, h is the nonlinear term or uncertainty parameter. Since (C, A) is observable, constant matrix L exists, and configuring to complex plane half, left-hand side of the following equation, A_o can have stable eigenvalue,

$$A_o = A - LC. \quad (13)$$

Therefore, there is

$$PA_0 + A_0^T P = -Q, \quad (14)$$

satisfying $P > 0$ for A_o and positive matrix $Q > 0$, and F can be defined as

$$FC = B^T P. \quad (15)$$

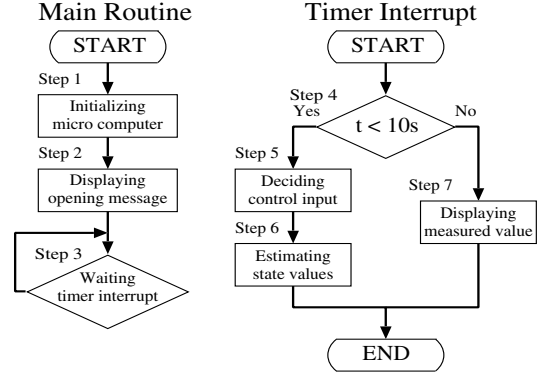


Fig. 7 Control algorithm.

State estimate error e is defined by

$$e(t) = \hat{x}(t) - x(t). \quad (16)$$

and F estimation error α is defined by

$$\alpha = F\{\hat{y}(t) - y(t)\}. \quad (17)$$

where, $\hat{x}(t)$ and $\hat{y}(t)$ are the estimated value of $x(t)$ and $y(t)$. Using these equations, the design of the VSS observer can be obtained.

$$\begin{aligned} \dot{\hat{x}}(t) &= A_0 \hat{x} + Ly + Bu + B\delta, \\ \delta(t) &= \begin{cases} -\frac{\alpha}{\|\alpha\|} \rho & \text{for } \alpha \neq 0, \\ 0 & \text{for } \alpha = 0. \end{cases} \end{aligned} \quad (18)$$

where, ρ is a constant. The following error equation can be obtained by differentiating Eq. (18).

$$\begin{aligned} \dot{e} &= \dot{\hat{x}} - \dot{x} \\ &= A_0 \hat{x} + Ly + Bu + B\delta - Ax - Bh - Bu \\ &= A_0 e + B\delta - Bh \\ &= \begin{cases} A_0 e - B \frac{\alpha}{\|\alpha\|} \rho - Bh & \text{for } \alpha \neq 0, \\ A_0 e - Bh & \text{for } \alpha = 0. \end{cases} \end{aligned} \quad (19)$$

It selects Lyapunov function V_o as following equation.

$$V_o = \frac{1}{2} e^T P e. \quad (20)$$

By differentiating V_o with respect to t , we have

$$\dot{V}_o = \frac{1}{2} e^T P \dot{e} + \frac{1}{2} e^T P \dot{e}, \quad (21)$$

where, by substituting Eq. (19), $FC = B^T P$, $e^T C^T F^T = \alpha^T$, and $|\alpha^T h| \leq \|\alpha\| \rho$, we have

$$\begin{aligned} \alpha \neq 0 \\ \dot{V}_o(t) &= \frac{1}{2} e^T (PA_0 + A_0^T P) e \\ &\quad - e^T P B \frac{\alpha}{\|\alpha\|} \rho - e^T P B h \\ &= -e^T Q e - e^T C^T F^T \frac{\alpha}{\|\alpha\|} \rho - e^T C^T F^T h \\ &= -e^T Q e - \|\alpha\| \rho - \alpha^T h \\ &\leq -e^T Q e - \|\alpha\| \rho + \|\alpha\| \rho = -e^T Q e, \end{aligned} \quad (22)$$

$$\begin{aligned} \alpha = 0 \\ \dot{V}_o(t) &= \frac{1}{2} e^T (PA_0 + A_0^T P) e - e^T P B h \\ &= -e^T Q e - \alpha^T h \\ &\leq -e^T Q e, \end{aligned} \quad (23)$$

which obtains $e(t) \rightarrow 0(t \rightarrow \infty)$ for \dot{V}_o .

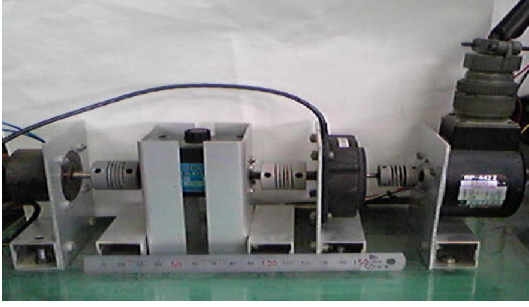


Fig. 8 Configuration of USM.

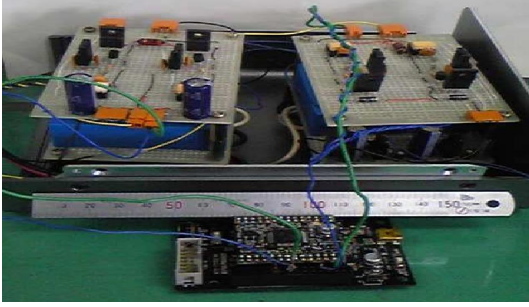


Fig. 9 Micro computer and drive circuit.

IV. EXPERIMENTAL RESULTS AND DISCUSSION

A. Micro computer algorithm

Micro computer used in this research is SH7125 of SH/Tiny series. It uses development environment tool HEW(High-performance Embedded Workshop) of Renesas Technology Corp, and is written in C. Features of SH7125 are PWM mode, timer interrupt, and phase number count mode of MTU2. Using these features, we implemented nonlinear controller for the USM.

The flow chart of the control algorithm is shown in Fig. 7, and the steps are given as following.

- STEP1 Initialize micro computer.
- STEP2 Display opening message.
- STEP3 Wait for timer interrupt.
- STEP4 Determine the setting time.
- STEP5 Decide the control input.
- STEP6 Estimate the state values.
- STEP7 Display the measured value.

B. Experimental Results

USM experimental set up is shown in Fig. 8, and the micro computer and the drive circuit are shown in Fig. 9. Here, control cycle is 1 ms, data sampling time is 20 ms, reference position of USM is sinusoidal wave, reference position frequency is 0.2 Hz, drive frequency f is 41 kHz, initial position is $y = 0.0$ rad and they are implemented digitally. Control parameters are shown in Table 2.

Experimental results by using the proposed nonlinear controller are shown in Figs. 10, and 11. Figs. 10(a), and 11(a), provide good control for both no load and applied load. Figs. 10(d), and 11(d), provide good

Table 2. Control parameters.

S	$[-1.1 \times 10^4 \quad 8.8 \times 10^3 \quad 147.7 \quad 3.2]$
K_f	3.3
k	0.1
F	1
ρ	0.1
L	$[0.3 \quad 1.4 \times 10^{-9} \quad -7.1 \times 10^{-5}]^T$
ζ	0.2
ω_n	2200.8

position estimation. Figs. 10(f), and 11(f) provide that quantization error is reduced in estimated speed.

Therefore, from the discussion of the experimental results, it can be said that the proposed nonlinear controller has robustness, provide effective control of the USM with unknown dead-zone.

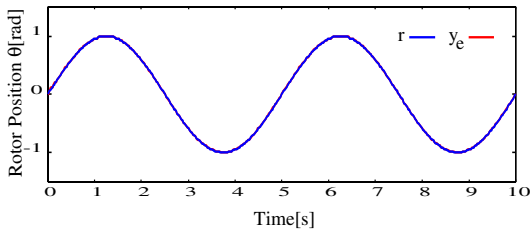
V. CONCLUSIONS

The USM has an excellent performance and many other useful features. However, dead-zone occurs in control input with applied torque. In this paper, we propose robust position control of the USM using the nonlinear controller considering dead-zone and the VSS observer. The nonlinear controller considering dead-zone achieves robust position control of USM. The VSS observer is a nonlinear observer, achieves reduction of quantization error and provides good position estimation.

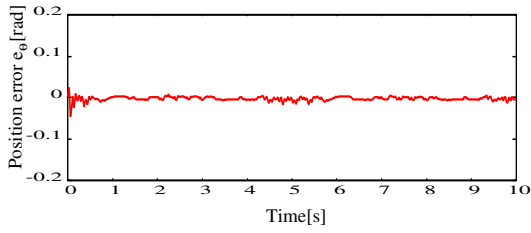
Then, the dead-zone effect is reduced by the nonlinear controller with the VSS observer. Experimental results demonstrated good tracking performance and robustness of the proposed control and estimation scheme.

REFERENCES

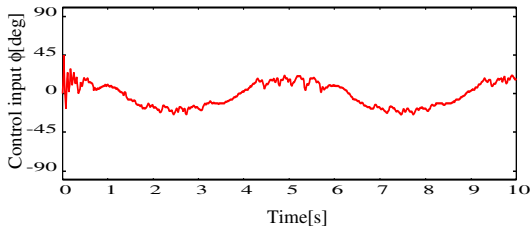
- [1] T. Kenjyo, and T. Sashida, "An Introduction of Ultrasonic Motor", Oxford Science Publications, 1993.
- [2] Tomohiro Yoshida, Tomonobu Senjyu, Mitsuru Nakamura, Atsushi Yona, Naomitsu Urasaki, and Hideomi Sekine, "Position Control of Ultrasonic Motors using Two-control Inputs H_∞ Controller", *Electric Power Components and Systems*, vol. 35, pp. 741-755, 2007.
- [3] Tomonobu Senjyu, Mitsuru Nakamura, Naomitsu Urasaki, Hideomi Sekine, and Toshihisa Funabashi, "Mathematical Model of Ultrasonic Motors for Speed Control", *Electric Power Components and Systems*, vol. 36, pp. 637-648, 2008.
- [4] Hyonyong Cho, and Er-Wei Bai, "Convergence Results for an Adaptive Dead Zone Inverse", *International Journal of Adaptive Control and Signal Processing*, vol. 12, pp. 451-466, 1998.
- [5] Xing-Song Wang, Chun-Yi Su, and Henry Hong, "Robust adaptive control of nonlinear systems with unknown dead-zone", *Automatica*, vol. 40, pp. 407-413, 2004.
- [6] Brice Beltran, Tarek Ahmed-Ali, and Mohamed El Hachemi Benbouzid, "Nonlinear Power Control of Variable-Speed Wind Energy Conversion Systems", *IEEE Trans. Energy Conversion*, vol. 23, pp. 551-558, 2008.
- [7] Yi-feng Chen, and Tsutomu Mita, "Sliding Mode Control with Adaptive VSS Observer", *T. IEE Japan*, vol. 111-C, pp. 514-522, 1991.
- [8] Liping Guo, John Y. Hung, and R. M. Nelms, "Digital Implementation of Nonlinear Fuzzy Controllers for Boost Converters", *Applied Power Electronics Conference and Exposition(APEC'06)*, pp. 1424-1429, 2006.
- [9] Hsu-Chih Huang, and Ching-Chih Tsai, "FPGA Implementation of an Embedded Robust Adaptive Controller for Autonomous Omnidirectional Mobile Platform", *IEEE Trans. Ind. Electron.*, vol. 56, pp. 1604-1616, 2009.
- [10] Da Zhang, and Hui Li, "A Stochastic-Based FPGA Controller for an Induction Motor Drive With Integrated Neural Network Algorithms", *IEEE Trans. Ind. Electron.*, vol. 55, pp. 551-561, 2008.



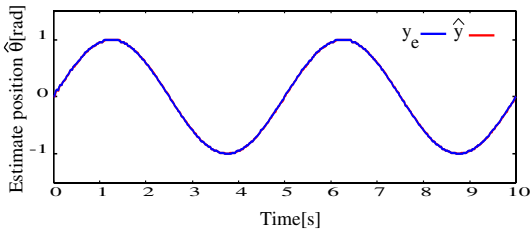
(a) Reference position and measured position.



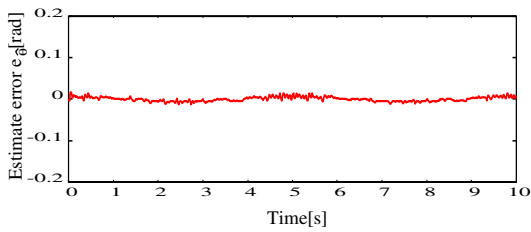
(b) Position error.



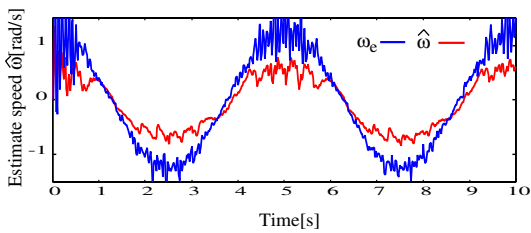
(c) Control input.



(d) Measured position and estimate position.

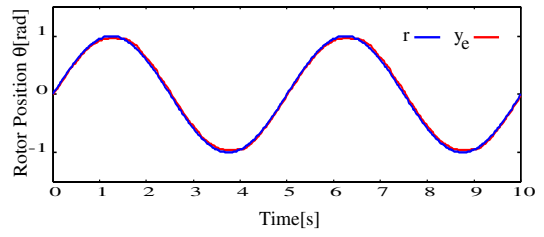


(e) Estimate position error.

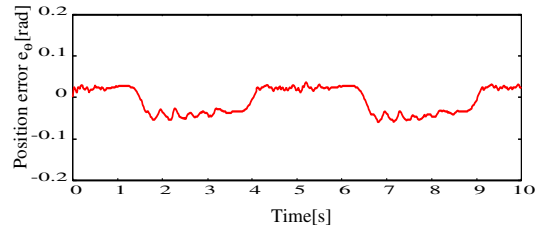


(f) Measured speed and estimate speed.

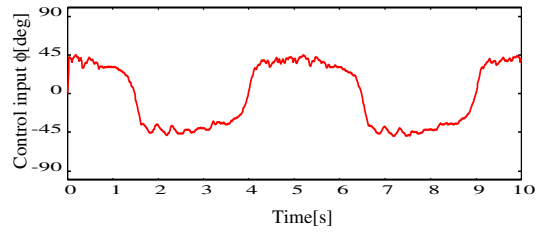
Fig. 10 Experimental result with nonlinear controller ($\tau_L=0.0\text{Nm}$).



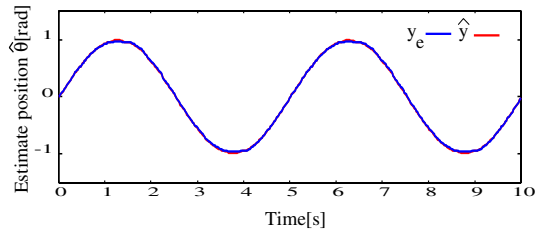
(a) Reference position and measured position.



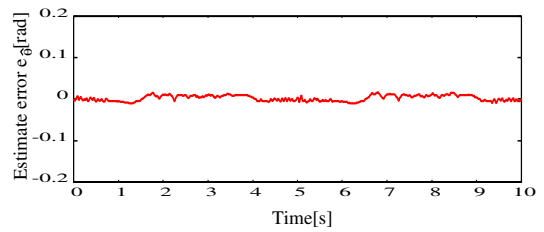
(b) Position error.



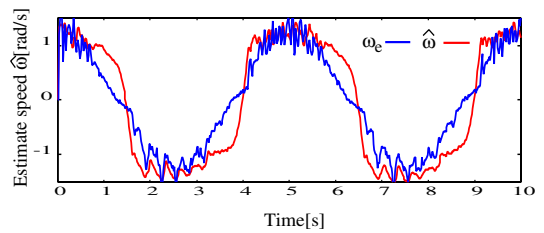
(c) Control input.



(d) Measured position and estimate position.



(e) Estimate position error.



(f) Measured speed and estimate speed.

Fig. 11 Experimental result with nonlinear controller ($\tau_L=0.2\text{Nm}$).